SLAC-PUB-10712
September 2004

ATTOSECOND X-RAY PULSES IN THE LCLS USING THE SLOTTED FOIL METHOD *

P. Emma†, Z. Huang, SLAC, Stanford, CA 94309, USA
M. Borland, ANL, Argonne, IL 60439, USA

Abstract

A proposal has been made to generate femtosecond and sub-femtosecond x-ray pulses in the Linac Coherent Light Source (LCLS) SASE FEL [1] by using a slotted spoiler foil located at the center of the second bunch compressor chicane [2]. This previous study highlighted a simple case, using the nominal LCLS parameters, to produce a 2-fsec FWHM, 8-keV x-ray pulse. The study also pointed out the possibility of attaining sub-femtosecond pulses by somewhat modifying the LCLS compression parameters, but did not undertake a full study for this more aggressive case. We take the opportunity here to study this 'attosecond' case in detail, including a full tracking simulation, exploring the limits of the technique.

INTRODUCTION

Within the community of synchrotron radiation users there is a rapidly growing interest in the availability of extremely short pulses as experimental probes in several fields of research, including structural studies of single biomolecules, x-ray diffraction from a single protein molecule, and femtosecond chemistry. The interest in sub-femtosecond (*i.e.*, attosecond [as] $= 10^{-18}$ sec) pulses lies in the fact that electron transfer reaction dynamics in atomic and molecular systems, providing information about the most basic reaction mechanisms in chemistry, biology, and soft/condensed matter physics, are on the femtosecond and sub-femtosecond time scales (see *e.g.*, [3]).

A previous study [2], based on the LCLS X-ray FEL, described the production of a 2-fs FWHM (full-width at half-maximum) long x-ray pulse generated by differentially spoiling the electron bunch by passing it through a thin slotted foil within the second magnetic bunch compressor chicane (see Fig. 1).

The method relies upon the fact that in a magnetic bunch-compressor chicane the beam is tilted at a large angle relative to the longitudinal axis t (or $z \approx ct$) as shown in Fig. 1. At the point of maximum tilt (center of the chicane) a thin foil is placed in the path of the beam. The foil has a vertically (y) oriented narrow slot at its center. The Coulomb scattering of the electrons passing through the foil increases the horizontal and vertical emittance of most of the beam, but leaves a very thin unspoiled slice where the beam passes through the slit. Spoiling the emittance of most of the beam by a factor of ~5 will strongly suppress the FEL gain for these sections, while the very short unspoiled time-slice will produce an x-ray FEL pulse much shorter than the full 200-fs FWHM electron bunch length.

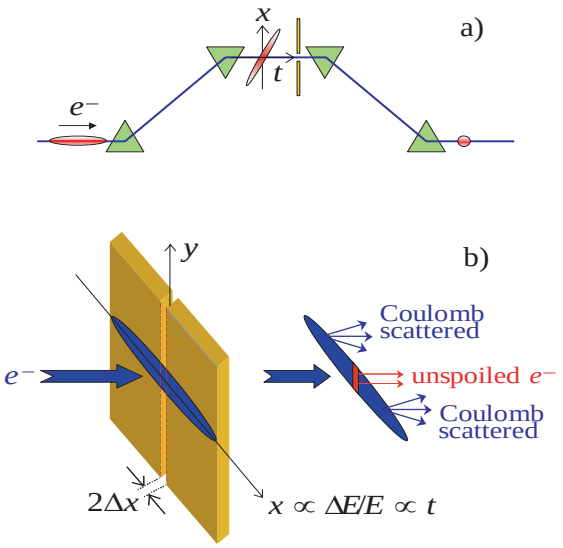

Figure 1: a) Sketch of electron bunch at center of magnetic bunch-compressor chicane with tilted beam in horizontal, x, and longitudinal coordinates, t. b) The slotted foil at chicane center generates a narrow, unspoiled beam center.

The previous study was based on the nominal LCLS machine parameters in order to highlight the compatibility of the technique with the baseline LCLS design. As briefly described therein, the pulse length can be further reduced by re-optimizing the operational machine parameters. We describe here the limiting pulse length of the unspoiled electrons and the necessary parameter adjustments to reach the limit, highlighting a detailed study which can produce a 400-as FWHM x-ray pulse duration using the LCLS design, but with a few changes to the operational configuration, such as an increased bunch compression factor and a reduced bunch charge, in order to avoid micro-bunching instabilities.

NOMINAL ACCELERATOR CONFIGURATION

Electron bunch length compression in the LCLS is accomplished in two stages. Each stage relies on an energy-chirped electron bunch passing through a magnetic chicane with energy-dependent path length. The chirp, h, is the slope of the relative energy variation along the bunch length coordinate, z_0, prior to the chicane, and is approximately

* This work is supported by the U.S. Department of Energy, contract DE-AC02-76SF00515.
† Emma@SLAC.Stanford.edu

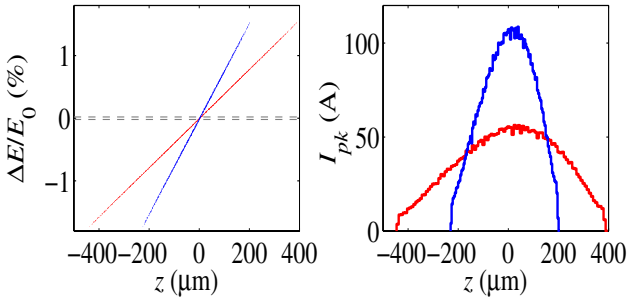

Figure 2: Chirped bunch (left) at start (red) and center (blue) of chicane with initial energy-chirp (red slope) of: $h \approx 39$ m^{-1}, and extremely narrow uncorrelated width. The foil slot is indicated as dashed lines and the current profiles are at right (100-pC case).

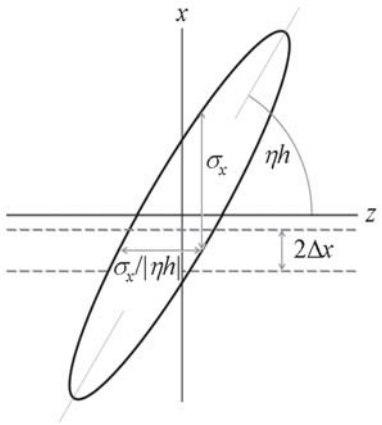

Figure 3: Energy-chirped (and therefore spatially-chirped) electron bunch at center of chicane.

equal to the total rms relative energy spread divided by the rms bunch length, as shown in Fig. 2 .

In the LCLS layout, the first bunch compressor chicane, BC1, is located at an energy of 250 MeV and nominally compresses the bunch length from 850 μm to 200 μm rms, while the second compressor is located at 4.5 GeV and compresses from 200 μm to 20 μm rms. The energy-dependent path length coefficient, or momentum compaction, of the BC2 is $R_{56} \approx -25$ mm, which describes the path length change for a particle with relative energy error: $\delta \equiv \Delta E/E_0$. The minus sign indicates that a high energy particle takes a shorter path, $\Delta z = R_{56}\delta$. The larger momentum dispersion, smaller uncorrelated energy spread, and smaller transverse beam size in the BC2 make this location the best choice for producing the shortest duration unspoiled electron pulse.

UNSPOILED ELECTRON PULSE LENGTH

The final unspoiled electron pulse duration is limited by several effects. The time-sliced rms horizontal betatron beam size at the foil (*i.e.*, $\sigma_{x_\beta} = \sqrt{\epsilon\beta}$, where ϵ is the horizontal beam emittance and β is the horizontal beta-function at the foil) limits the width of the slit (see σ_x in Fig. 3). The slit half-width, Δx, should be larger than, or similar to, approximately 3-times the betatron beam size (*i.e.*, $\Delta x \gtrsim 3\sqrt{\epsilon\beta}$), otherwise the peak current will be cut, and the FEL gain of the spike will be reduced. Similarly, the beam size in the slit has a contribution from the intrinsic (uncorrelated) rms relative energy spread (increased by ~ 2 due to half compression at the slit) times the chicane's dispersion at the foil (*i.e.*, $\Delta x \gtrsim 6|\eta|\sigma_{\delta_0}$), although this contribution to beam size is typically not significant. These contributions determine the minimum slit width that will not cut the peak current.

The minimum length of the unspoiled section of the electron bunch can be calculated in the following way, assuming ultra-relativistic electrons. The final bunch length coordinate (after the chicane), z, is expressed in terms of the initial bunch length coordinate (prior to the chicane), z_0, the chicane's momentum compaction, R_{56}, the bunch energy-chirp prior to the chicane, h, and the initial uncorrelated relative energy deviation of the particle, δ_0.

$$z = z_0 + R_{56}(hz_0 + \delta_0) = (1 + hR_{56})z_0 + R_{56}\delta_0 \quad (1)$$

Similarly, the transverse extent of the beam at the foil, x, can be written in terms of the momentum dispersion at the foil, η, the betatron component of the transverse coordinate, x_β, and the energy-chirp, h.

$$x = x_\beta + \eta(hz_0 + \delta_0) \quad (2)$$

Solving Eq. (1) for z_0 and inserting this into Eq. (2) gives

$$x = (1 + hR_{56})x_\beta + h\eta z + \eta\delta_0. \quad (3)$$

From Fig. 3 the length of the unspoiled section of electrons is a minimum when the slit width, Δx, approaches zero (temporarily ignoring the loss of peak current as described above). This is arranged by simply setting Eq. (3) to zero (with the slit at $x = 0$) and solving for z.

$$z = -\frac{\delta_0}{h} - \frac{(1 + hR_{56})x_\beta}{h\eta} \quad (4)$$

Since x_β and δ_0 are by definition uncorrelated, the rms length of the unspoiled bunch, $\langle z^2\rangle^{1/2} = \sigma_{z_u}$, for a zero slit width, is then

$$\sigma_{z_u} = \frac{1}{|\eta h|}\sqrt{\eta^2\sigma_{\delta_0}^2 + (1 + hR_{56})^2\sigma_{x_\beta}^2}, \quad (5)$$

where σ_{δ_0} is the initial rms uncorrelated relative energy spread at the start of the chicane and $\sigma_{x_\beta} = \sqrt{\epsilon\beta}$ is the rms betatron beam size at the foil.

From Fig. 3 the contribution to this length from a finite slit width is the rms of the nearly uniform x-distribution

in the slit, $\Delta x/\sqrt{3}$, converted to the z-direction by $1/|\eta h|$, and added in quadrature to the betatron beam size term in Eq. (5). Therefore, the FWHM duration of the unspoiled portion of the electron bunch is given by

$$\Delta\tau \approx \frac{2.35}{|\eta h|c}\sqrt{\eta^2\sigma_{\delta_0}^2 + (1+hR_{56})^2\left[\Delta x^2/3 + \epsilon\beta\right]}, \quad (6)$$

where c is the speed of light and $2.35 \approx 2\sqrt{2\ln(2)}$.

Equation (6) shows that an increased energy-chirp value, $|h|$, provides a shorter unspoiled pulse. It is also clear that the betatron beam size, $\sqrt{\epsilon\beta}$, and the slit half-width, Δx, are both effectively compressed by the inverse of the bunch compression factor: $1/C \equiv |1+hR_{56}| \ll 1$. The uncorrelated energy spread term, $\eta\sigma_{\delta_0}$, however, is not compressed and typically sets the minimum length limit. This small energy spread is established in the electron gun where it has been measured at about 3 keV rms [4], which agrees well with computer simulations. The 3-keV energy spread is amplified linearly by the bunch compression factor of the BC1. In the case of the LCLS, it is increased by a factor of 4.5, to 13.5 keV, which at 4.54 GeV, prior to the BC2, is an extremely small rms relative energy spread of $\sigma_{\delta_0} \approx 3\times10^{-6}$.

This very small local energy spread can allow various micro-bunching instabilities to develop in the linac [5] by providing no effective Landau damping in the chicanes. In fact, the LCLS design includes a beam heater system to increase the local energy spread to 40 keV (prior to BC1 compression) to Landau damp the micro-bunching instabilities. This increased energy spread, however, excludes the possibility to generate sub-femtosecond pulses using the slotted-spoiler foil, and leads to the 2-fs FWHM x-ray pulse discussed in reference [2]. For this reason, we propose a greatly reduced bunch charge of 100 pC for this sub-femtosecond application (rather than 1 nC in [2]). This reduced charge, and proportionally reduced peak current in the linac sections leading to BC2, moderates the instability and allows the preservation of this very small local energy spread from the RF photo-injector gun, thus enabling sub-femtosecond pulse generation with the foil.

ACCELERATOR PARAMETERS AND ISSUES

For this low charge (100 pC), we assume a transverse normalized emittance of $\gamma\epsilon_{x,y} \approx 0.5$ μm is possible (rather than the nominal level of 1 μm at 1 nC); a level which seems fairly conservative given the factor of ten charge reduction. In addition, the linac RF phases and voltage levels are necessarily adjusted to compensate for the reduced longitudinal wakefields in the accelerating structures, but in this example the initial bunch length is unchanged, the BC1 and BC2 chicane strengths are not altered, and the compression factor of 4.5 in the BC1 is maintained. Because of the factor of 10 charge (and current) reduction compared to the standard LCLS design, the microbunching instability driven by longitudinal space charge and coherent synchrotron radiation without the beam heater (assuming only 3 keV initial uncorrelated rms energy spread) is very mild. For example, for any initial beam modulation wavelength $\lambda > 50$ μm, we estimate that $\pm$ 1% density modulation at the end of the injector can cause no more than 0.7×10^{-6} rms energy modulation at the BC2 entrance, which adds insignificantly to the intrinsic beam energy spread $\sigma_{\delta_0} \approx 3\times10^{-6}$. Nevertheless, the temporal profile of the photocathode drive laser should be sufficiently smooth in order to not introduce any excessive beam density modulation. A Gaussian laser profile instead of a flattop profile might be preferable for this attosecond x-ray generation since only the emittance of the Gaussian core needs to be about 0.5 μm.

Table 1: LCLS BC2 chicane and beam parameters.

Parameter	**symbol**	**value**	**unit**
bunch charge	Q	100	pC
chicane energy	E_0	4.54	GeV
chicane dispersion	η	363	mm
momentum compaction	R_{56}	-24.7	mm
energy chirp	h	39.0	1/m
rms initial E-spread	σ_{δ_0}	3	10^{-6}
beta at foil	β	8.0	m
normalized emittance	$\gamma\epsilon$	0.5	μm
length of each bend	L_B	0.50	m
angle of each bend	$\lvert\theta_B\rvert$	1.98	deg

Table 1 lists the BC2 chicane and beam parameters used to generate a sub-femtosecond x-ray pulse. Using these parameter values, Fig. 4 shows Eq. (6) plotted (blue) versus the slit half-width, Δx, along with an almost identical (red) curve from particle tracking. The dash-dot curve (green) includes the local energy spread generated from incoherent synchrotron radiation in the chicane dipoles (3.6×10^{-6} rms per 0.5-m long, 2-degree bend at 4.54 GeV), which is not included in Eq. (6). The parameters in Table 1, and a 70-μm slit half-width ($=\Delta x$), chosen to preserve at least 1.3 kA of peak current, will produce a FWHM unspoiled electron pulse of 1.3 fs. This will be 'gain-narrowed' in the FEL producing a FWHM x-ray pulse as short as 400 as, while the spoiled beam has transverse emittance levels of $\gamma\epsilon_{x,y} \approx 6$ μm and does not produce FEL radiation.

TRACKING SIMULATIONS

To test these parameters and better estimate the final x-ray pulse length, the entire LCLS is simulated with three consecutive particle tracking computer codes: *Parmela* [6], *Elegant* [7], and *Genesis 1.3* [8]. The tracking includes space-charge forces in the RF photo-cathode gun and low-energy injector systems (*Parmela*), 2nd-order optics, wakefields, and coherent synchrotron radiation (CSR) in the dipole magnets (*Elegant*), and time-dependent FEL exponential gain and saturation in the undulator (*Genesis 1.3*).

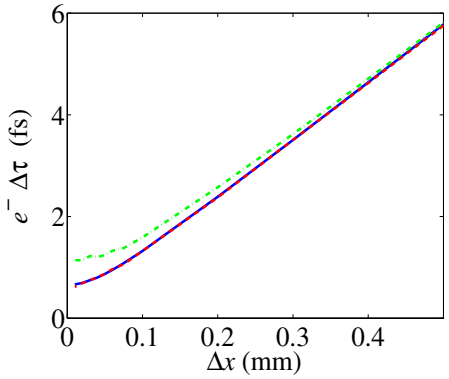

Figure 4: FWHM unspoiled e^- bunch duration as a function of slit half-width, Δx. The blue (solid) curve is Eq. (6), the red (dashed) is from particle tracking, and the green (dash-dot) is tracking which includes synchrotron radiation in the dipoles.

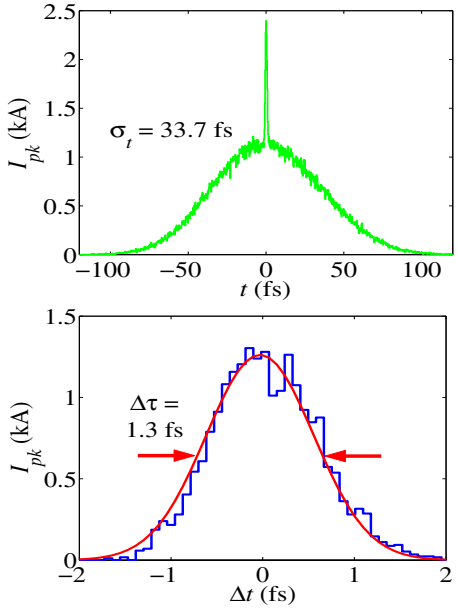

Figure 5: Current profile after BC2 (top) with spike created by e^- passing through the slit, and unspoiled e^- only (bottom) after BC2 with 1.3-fs FWHM and 1.3 kA.

Although the possibility of <0.5-μm emittance at 100 pC was verified [9] with *Parmela*, for convenience, a 1-nC run was used and each particle's action was scaled to produce a 0.5-μm core emittance.

As seen at the top plot in Fig. 5, the narrow section of electrons which pass through the slit produce a sharp spike on the current profile after the BC2 chicane. This spike is the result of electrons near the edge of the slit scattering in the foil. The scattering generates a slightly different path length for the electrons through the last half of the chicane and causes a small time-smearing inside the bunch according to

$$\Delta\sigma_t \approx |\eta|\sigma_\theta/c, \tag{7}$$

where σ_θ is the rms Coulomb scattering angle (22 μrad) through a 50-μm thick Be foil. Some of the scattered electrons then overlap in time with the unspoiled time-slice, raising the local peak current, and creating both an unspoiled core (the electrons that pass through the slit) and a spoiled halo (the time-smeared electrons from near the edge of the slit). The FEL process amplifies only the cold beam core and is unaffected by the halo. This sharp spike, however, can potentially damage the bend-plane emittance through CSR effects, which is a further reason to choose a very low bunch charge of 100 pC. Calculations with a line-charge (1D) CSR model (50-nm bin size) indicate very little emittance growth (<2%) in the unspoiled electrons through all LCLS bend magnets beyond the foil, partially due to the large tilted transverse beam size in the bends.

The Coulomb-scattered time smearing also keeps the peak current of the full bunch below 1.5 kA (not including the spike), limiting the possible CSR-induced beam brightness degradation from the full beam. Without this time-smearing, the peak current may approach 10 kA and the beam may break up in the chicanes.

The Coulomb scattering in the foil is simulated in *Elegant*, which includes a model for very thin foils with thickness $<10^{-3}$ of its radiation length [10]. The 50-μm thick Beryllium foil is $\sim 10^{-4}$ of its radiation length ($X_0 \approx 35$ cm), and the angular distribution produced by *Elegant* agrees well with theoretical calculations for very thin foils [11].

Finally, a model for the transition radiation wakefield [12] of the foil, but ignoring the slot, has been included in previous simulations [2] at 1-nC of charge and was found to have an insignificant effect on the unspoiled beam. In this case, at only 100-pC of total charge, the time-consuming simulation of the wakefield is not included here.

The bottom plot in Fig. 5 shows only the unspoiled electrons after the chicane with a FWHM duration of 1.3 fs and 1.3-kA of peak current with 1.8-pC of charge. The emittance of these unspoiled electrons is $\gamma\epsilon_{x,y} \approx 0.4$ μm (smaller than 0.5 μm because they are taken from the cold core of the *Parmela*-generated distributions). Their relative rms energy spread at 14.3 GeV is 6×10^{-5}, including the effects of CSR. It is also estimated, but not included in tracking, that the longitudinal space-charge forces in the 1100-m of linac and transport lines beyond the BC2 chicane will generate an additional rms energy spread of $<10^{-4}$ within this unspoiled electron section, which should increase the FEL gain length by <5%. Similarly, the resistive-wall longitudinal wakefield in a 100-m long undulator with radius 2.5 mm and copper surface, produces an insignificant rms energy spread of $< 2 \times 10^{-5}$. The tracked particles, both spoiled and unspoiled, are transferred to the FEL code *Genesis 1.3* for a time-dependent FEL simulation.

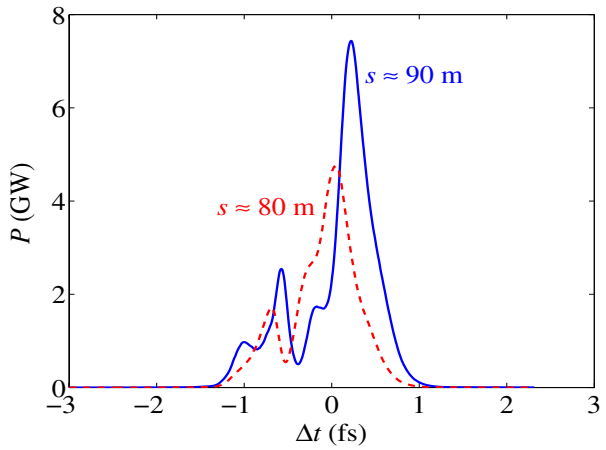

Figure 6: X-ray power profile at $s \approx 80$ m (red-dash) and $s \approx 90$ m (blue-solid) along the undulator, with 570-as (80 m) and 380-as (90 m) FWHM spike duration at 5-7 GW.

FEL SIMULATIONS

The FEL performance is simulated using *Genesis 1.3* [8] with parameters as listed in Table 2. Only a time window of about 6 fs containing the unspoiled 1.3-fs electrons is used in the simulation, since the spoiled electrons do not participate in the FEL interaction as shown in ref. [2]. The FEL interaction with the unspoiled electrons saturates around 80 m, with the radiation pulse further narrowed from the unspoiled electron pulse due to the nonlinear interaction. The x-ray power profile is shown in Fig. 6 at both 80 and 90 meters along the undulator. The pulse at 90 m has a 380-as FWHM duration with 7-GW of peak power and $\sim 2\times 10^9$ 8-keV photons in this one spike.

Table 2: LCLS FEL Parameters.

Parameter	symbol	value	unit
electron energy	E_0	14.3	GeV
radiation wavelength	λ_r	1.5	Å
undulator parameter	K	3.71	
undulator period	λ_u	3	cm
mean beta function	$\langle\beta\rangle$	30	m

STABILITY AND SYNCHRONIZATION

In a real operating machine, the beam energy, timing, and charge will vary from shot to shot, as will RF phases and amplitudes of the various linac sections. If the beam energy centroid changes prior to the BC2 chicane, the mean horizontal beam position in the slot will also change. This may affect the peak current and pulse width of the unspoiled electron pulse, as well as the final bunch arrival time in the FEL undulator.

To estimate these levels, 1000 2D-tracking runs were performed (ignoring transverse variations) to simulate an

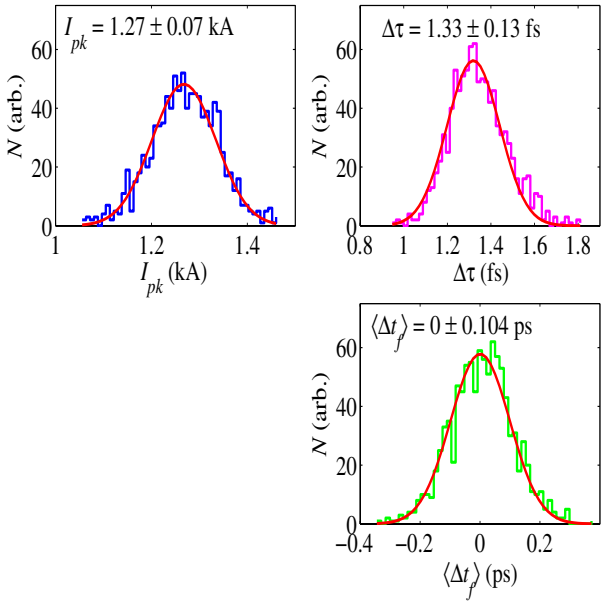

Figure 7: Peak current (top-left), FWHM unspoiled e^- pulse width (top-right), and bunch arrival time (bottom-right) variation over 8-sec of LCLS operation at 120 Hz, using rms machine jitter levels given in Table 3.

8-second span of LCLS operation at 120 Hz. Each beam or machine parameter in Table 3 is randomly varied in a Gaussian distribution with rms value as listed (1 deg-S $\approx$ 1 ps). The RF phase and amplitude errors are applied independently to each of the 5 main linac sections (see ref. [1], Ch. 7, pg. 7-28, Table 7.10). The tracking also includes the effects of charge-dependent longitudinal wakefields. The final unspoiled beam energy, arrival time, peak current, and pulse width, are then recorded to estimate the stability of the unspoiled beam.

Table 3: Expected short-term machine jitter levels (rms).

Parameter	symbol	value	unit
Relative bunch charge	$\Delta Q/Q$	2	%
Drive laser-gun timing	Δt_g	0.5	ps
RF phase of each linac	ϕ_{RF}	0.1	deg-S
RF amp. of each linac	$\Delta V/V$	0.1	%

The fixed slot position determines the energy of the unspoiled beam, after the chicane, to a very high degree, but the peak current, arrival time, and pulse width vary as shown in Fig. 7. Although the relative peak current and pulse width each vary by $<$10% rms, the final bunch arrival time varies by 100 fs rms, which is quite large in comparison to the 400-as pulse width. This is one clear limitation of this method, where pump-probe experiments may have to measure this timing variation in order to meaningfully 'time-bin' the data collection. Longer term machine variations will be stabilized by beam feedback systems.

REFERENCES

[1] LCLS Conceptual Design Report, SLAC-R-593 (2002), http://www-ssrl.slac.stanford.edu/lcls/cdr/.

[2] P. Emma et al., *Femtosecond and Sub-Femtosecond X-ray Pulses from a SASE-Based Free-Electron Laser*, Phys. Rev. Lett. 92:074801, (2004).

[3] R. Neutze et al., Nature **406** 752-757 (2000); M. Drescher et al., *ibid.* **419** 803-807 (2002).

[4] M. Hüning and H. Schlarb, *Measurement of the Beam Energy Spread in the TTF Photoinjector*, Proc. of the 2003 Particle Acc. Conf., Portland, OR (IEEE, Piscataway, NJ, 2003).

[5] Z. Huang et al., *Suppression of Microbunching Instability in the Linac Coherent Light Source*, Phys. Rev. ST Accel. Beams 7:074401 (2004).

[6] J. Billen, *PARMELA*, Los Alamos National Laboratory Report LA-UR-96-1835 (1996).

[7] M. Borland, APS LS-287, Sep. 2000.

[8] S. Reiche et al., Nucl. Instrum. & Methods, **A483** (2002) 70.

[9] C. Limborg, private communication, June 2004.

[10] M. Borland, ANL/APS, OAG-TN-2003-007, 2003.

[11] W.R. Leo, *Techniques for Nuclear and Particle Physics Experiments*, (Springer-Verlag, Berlin, 1994).

[12] K.L.F. Bane and G. Stupakov, *Transition Radiation Wakefields for a Beam Passing through a Metallic Foil*, SLAC-PUB-9726, June 2003.